Original Article | Gastrointestinal Imaging

eISSN 2005-8330
https://doi.org/10.3348/kjr.2020.1262
Korean J Radiol 2021;22(7):1077-1086

Korean Journal of Radiology
KJR

Quantitative Ultrasound Radiofrequency Data Analysis for the Assessment of Hepatic Steatosis in Nonalcoholic Fatty Liver Disease Using Magnetic Resonance Imaging Proton Density Fat Fraction as the Reference Standard

Sun Kyung Jeon[1], Jeong Min Lee[1, 2], Ijin Joo[1], Sae-Jin Park[1, 3]

[1]Department of Radiology, Seoul National University Hospital, Seoul National University College of Medicine, Seoul, Korea; [2]Institute of Radiation Medicine, Seoul National University Medical Research Center, Seoul, Korea; [3]Department Radiology, SMG-SNU Boramae Medical Center, Seoul, Korea

Objective: To investigate the diagnostic performance of quantitative ultrasound (US) parameters for the assessment of hepatic steatosis in patients with nonalcoholic fatty liver disease (NAFLD) using magnetic resonance imaging proton density fat fraction (MRI-PDFF) as the reference standard.

Materials and Methods: In this single-center prospective study, 120 patients with clinically suspected NAFLD were enrolled between March 2019 and January 2020. The participants underwent US examination for radiofrequency (RF) data acquisition and chemical shift-encoded liver MRI for PDFF measurement. Using the RF data analysis, the attenuation coefficient (AC) based on tissue attenuation imaging (TAI) (AC-TAI) and scatter-distribution coefficient (SC) based on tissue scatter-distribution imaging (TSI) (SC-TSI) were measured. The correlations between the quantitative US parameters (AC and SC) and MRI-PDFF were evaluated using Pearson correlation coefficients. The diagnostic performance of AC-TAI and SC-TSI for detecting hepatic fat contents of ≥ 5% (MRI-PDFF ≥ 5%) and ≥ 10% (MRI-PDFF ≥ 10%) were assessed using receiver operating characteristic (ROC) analysis. The significant clinical or imaging factors associated with AC and SC were analyzed using linear regression analysis.

Results: The participants were classified based on MRI-PDFF: < 5% (n = 38), 5–10% (n = 23), and ≥ 10% (n = 59). AC-TAI and SC-TSI were significantly correlated with MRI-PDFF (r = 0.659 and 0.727, p < 0.001 for both). For detecting hepatic fat contents of ≥ 5% and ≥ 10%, the areas under the ROC curves of AC-TAI were 0.861 (95% confidence interval [CI]: 0.786–0.918) and 0.835 (95% CI: 0.757–0.897), and those of SC-TSI were 0.964 (95% CI: 0.913–0.989) and 0.935 (95% CI: 0.875–0.972), respectively. Multivariable linear regression analysis showed that MRI-PDFF was an independent determinant of AC-TAI and SC-TSI.

Conclusion: AC-TAI and SC-TSI derived from quantitative US RF data analysis yielded a good correlation with MRI-PDFF and provided good performance for detecting hepatic steatosis and assessing its severity in NAFLD.

Keywords: *Ultrasonography; Liver; Fatty liver; Nonalcoholic fatty liver disease; Quantitative imaging*

Received: October 20, 2020 **Revised:** November 11, 2020 **Accepted:** November 16, 2020

This study was supported by a research grant from Samsung Medison Co., Ltd (06-2018-4010) and a grant from the SNUH research fund (03-2018-02-30).

Corresponding author: Jeong Min Lee, MD, Department of Radiology, Seoul National University Hospital, Seoul National University College of Medicine, 101 Daehak-ro, Jongno-gu, Seoul 03080, Korea.

• E-mail: jmsh@snu.ac.kr

INTRODUCTION

Nonalcoholic fatty liver disease (NAFLD) affects approximately a quarter of the human population globally, with the earliest and characteristic histological features of hepatic steatosis [1]. NAFLD may progress to nonalcoholic steatohepatitis (NASH), an advanced form found in 20% of NAFLD patients [2,3]; NASH is a leading cause of liver transplantation as it can contribute to the development of fibrosis, cirrhosis, and hepatocellular carcinoma [2,4]. Liver biopsy is the current reference standard for diagnosing NAFLD; however, owing to its invasiveness and the possibility of sampling errors, a noninvasive technique is required for assessing hepatic steatosis [5].

Chemical shift-encoded magnetic resonance imaging (MRI)-based proton density fat fraction (PDFF) and magnetic resonance spectroscopy (MRS) are accurate and reproducible for liver fat quantification, and they are used as the validated reference standards in several clinical trials for NAFLD [6-8]. Despite their strengths, MRI-PDFF and MRS are not routinely performed for clinical screening of NAFLD because of cost-ineffectiveness. In this context, ultrasound (US) could be promising, as it is noninvasive, widely available, and cost-effective for the evaluation of hepatic steatosis [9]. B-mode US imaging, based on the amplitude of the envelope of beamformed radiofrequency (RF) signals, is frequently used clinically for the assessment of hepatic steatosis [10]. However, conventional B-mode US examination is limited by its subjectivity, operator dependency, and low sensitivity for mild steatosis [11].

Recently, quantitative US (QUS) techniques from RF data analysis have been proposed as noninvasive and objective tools for the detection and grading of hepatic steatosis. In recent years, various QUS techniques using non-image-based parameters, including speed of sound, US attenuation, backscatter coefficient, and shear-wave dispersion, have been proposed for assessing hepatic steatosis, and they have shown a significant correlation with hepatic steatosis [10,12-14]. In our previous study, we demonstrated that two QUS techniques (tissue attenuation imaging [TAI] and tissue scatter-distribution imaging [TSI]) showed good diagnostic performance for detecting hepatic steatosis in patients with chronic liver disease [15]. However, little is known about the diagnostic performance of these QUS parameters for detecting hepatic steatosis in patients with NAFLD.

Therefore, the purpose of our study was to investigate the diagnostic performance of QUS parameters for the assessment of hepatic steatosis in patients with NAFLD using MRI-PDFF as the reference standard.

MATERIALS AND METHODS

This single-center prospective study was approved by our Institutional Review Board, and written informed consent was obtained from all participants (ClinicalTrials.gov identifier: NCT04180631).

Study Population

Between March 2019 and January 2020, 124 participants who met the eligibility criteria and provided written informed consent were initially enrolled in this study. The inclusion criteria were as follows: 1) age of 18 years or older, 2) having been referred to the radiology department for ultrasonographic evaluation of the liver for known or suspected NAFLD or having been scheduled to undergo hepatectomy for liver donation. The exclusion criteria were as follows: 1) presence of clinical, laboratory, or histological evidence of liver disease other than NAFLD; 2) excessive alcohol consumption (≥ 14 and ≥ 7 drinks per week for male and female, respectively); 3) the use of hepatotoxic or steatogenic medication; 4) previous liver surgery; 5) contraindication for MRI; 6) missing MRI or QUS data. After excluding patients who had withdrawn consent (n = 1) and those with incongruencies in their data collected (n = 3), a total of 120 participants {75 male and 45 female; mean age, 49.1 years ± 12.6 (standard deviation [SD]); age range, 20–73 years} were finally included in this study (Fig. 1).

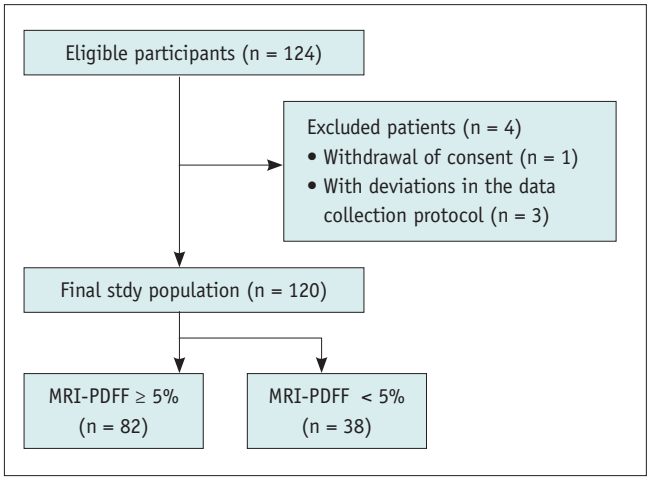

Fig. 1. Flowchart of the study population. MRI-PDFF = magnetic resonance imaging-proton density fat fraction

https://doi.org/10.3348/kjr.2020.1262

Korean Journal of Radiology
KJR

US Data Acquisition

For each participant, B-mode liver US examination was performed using a US system (RS 85, Samsung Medison, Co. Ltd.) with a convex probe (CA1-7A) by one of the three abdominal radiologists (with more than 6 years of experience in abdominal US examinations) who were blinded to the results of other studies. All participants were requested to fast for at least 4 hours before the US examinations. Each participant underwent two same-day sessions of examination to assess the reproducibility of the measurements of QUS parameters.

During each session of US examination, a radiologist performed six data acquisitions at the same location in the right lobe of the liver by using a right intercostal plane near the hepatic hilum. During the data acquisitions, the participants were placed in the supine position with the right arm maximally abducted. Each B-mode image was obtained during a breath-hold with a fixed set of time-gain compensations and positions of focus, and its RF data were automatically recorded.

During the B-mode US examination, the visual scores of hepatic steatosis were recorded by the operator as follows: 0, no steatosis; 1, mild steatosis; 2, moderate steatosis; 3, severe steatosis. They were based on Hamaguchi's scoring system using the following features: bright liver, increased hepatorenal echo contrast, deep attenuation, and vessel blurring [16]. In addition, the skin-to-liver capsular distance (mm) was measured by the operator

QUS Parameter Measurement

Two QUS parameters, including the attenuation coefficient (AC) at TAI (AC-TAI) and scatter-distribution coefficient (SC) at TSI (SC-TSI), were computed from the RF data using an in-house program developed in MATLAB R2015a (MathWorks, Inc.). By analyzing the RF data, the color-coded maps of both AC-TAI and SC-TSI of the corresponding B-mode images were generated (Fig. 2). The theoretical backgrounds of these two parameters are provided in Supplementary Material 1. Regarding B-mode images, one radiologist placed annulus-sector region of interests (ROIs) (approximately 2 cm for the inner arc length x 4 cm for side length) on TAI and TSI maps of the liver parenchyma by carefully avoiding large vessels, focal lesions, and reverberation artifacts under the liver capsule. When the blood vessels were unavoidable during ROI demarcation, demarcation, the areas containing large vessels were excluded from the calculation of AC-TAI and SC-TSI; those areas were vacant on the TAI and TSI maps. The measurements of QUS parameters were performed without knowledge of the MRI-PDFF results. For each QUS parameter, the six measurements for each examination were averaged. The results of the two sessions were used for reproducibility analysis; however, only the first session was used for steatosis assessment as the representative value for each participant.

MRI-PDFF and MR Elastography

All participants underwent chemical shift-encoded liver MRI with MR elastography (MRE) examinations using a 3T MR scanner (Skyra; Siemens Healthineers). For PDFF, complex-based chemical shift-encoded water-fat reconstruction techniques were used with six two-dimensional (2D) gradient-recalled-echo (GRE) images,

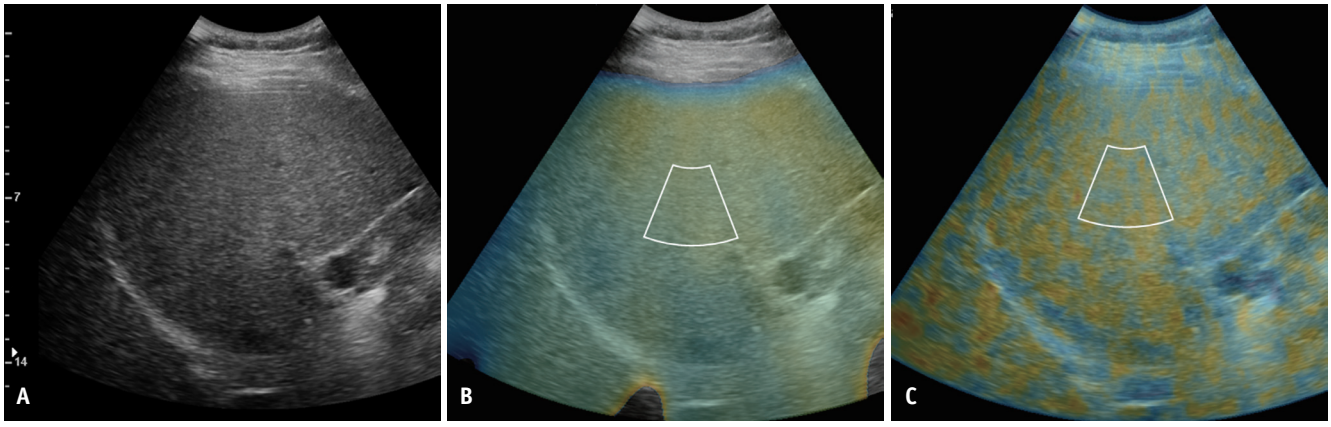

Fig. 2. Quantitative ultrasound parameters of radiofrequency data analysis.
From the acquired radiofrequency data of the B-mode ultrasound image **(A)**, the color-coded maps of TAI map reflecting center frequency **(B)** and TSI map reflecting Nakagamia parameters **(C)** are generated. With reference to the B-mode image, the annulus-sector region of interests were demarcated on the TAI map **(B)** and the TSI map **(C)**. The attenuation coefficient at TAI and the scatter-distribution coefficient at TSI were obtained. TAI = tissue attenuation imaging, TSI = tissue scatter-distribution imaging

https://doi.org/10.3348/kjr.2020.1262

an imaging matrix of 256 x 192, and a slice thickness of 3 mm. To minimize the T1 bias between fat and water, a low flip angle (4°) was used [17]. The PDFF maps were reconstructed automatically using the vendor's algorithm with T2* correction calculated from signal decay and a multi-peak fat model [18].

Blinded to the QUS results, one abdominal radiologist manually demarcated circular ROIs in each of the nine Couinaud liver segments of the PDFF map of each participant. Each ROI with a diameter of 1 cm was placed near the center of each segment to avoid large vessels, focal lesions, and artifacts. Nine ROIs were averaged and used as the reference standard for hepatic fat content [19]. The primary outcome was hepatic fat content of ≥ 5%, defined as MRI-PDFF of ≥ 5% [12,20]. In addition, hepatic fat contents of ≥ 10%, defined as MRI-PDFF of ≥ 10%, was the secondary outcome of our study [12,21].

MRE was also performed using a 2D GRE sequence in all participants; they were placed in the supine position with 60 Hz vibration applied to the abdominal wall. Four sections were acquired in four consecutive breath-holds. By using a direct inversion algorithm, a confidence mask was automatically generated from the scanner and superimposed on an MR elastogram [22]. Liver stiffness (LS) was measured by one abdominal radiologist by drawing a freehand ROI, excluding the large vessels, fissures, and focal liver lesions, in each section [23]. The LS values of each participant were expressed as the averages of stiffness values for each section (in kilopascals, kPa). Detailed imaging parameters of the MRE are provided in Supplementary Material 2.

To discriminate between various METAVIR fibrosis stages at MRE, we used the cutoff values suggested in a previous study [24]: 0–2.88 kPa for F0 (no fibrosis), > 2.88 kPa for ≥ F1 (mild fibrosis), > 3.54 kPa for ≥ F2 (significant fibrosis), > 3.77 kPa for ≥ F3 (advanced fibrosis), > 4.09 kPa for F4 (cirrhosis).

Statistical Analyses

Data are expressed as mean ± SD or number (percentage), as appropriate. Pearson correlation coefficients were used to assess the correlation between QUS parameters and MRI-PDFF. As the Kolmogorov-Smirnov test rejected the normality of the QUS parameters, the different steatosis grades assessed with MRI-PDFF were compared using the Kruskal-Wallis test. Following this, a Bonferroni-adjusted *p* value of less than 0.025 (0.05/2) was considered to indicate statistical significance during the Dunn post-hoc test, as two pairwise comparisons of adjacent grades were made. Receiver operating characteristic (ROC) curve analyses were used to assess the diagnostic performance of QUS parameters and the visual steatosis grades for detecting hepatic fat content of ≥ 5% (MRI-PDFF ≥ 5%) and ≥ 10% (MRI-PDFF ≥ 10%). For each ROC analysis, the area under the ROC curve (AUC), optimal cutoff values, and the following performance parameters were calculated: sensitivity, specificity, positive predictive value, and negative predictive value. The optimal cutoff value of each QUS parameter was determined using the Youden index [25]. The performance parameters of the visual steatosis grades were calculated based on the visual scores (≥ S1 [mild] and ≥ S2 [moderate], respectively). Pairwise comparisons of the AUCs of the QUS parameters and the visual steatosis grades were performed using Delong's test, with a Bonferroni-adjusted *p* value of less than 0.017 (0.05/3) indicating statistical significance. Inter-examination repeatability was evaluated using intra-class correlation coefficients (ICCs) and interpreted as follows: ≥ 0.90, excellent; 0.75–0.90, good; 0.50–0.75, moderate; < 0.50, poor reliability [26]. The coefficient of variation (CV), which is the ratio of the SD to the mean, was also calculated to provide an additional estimate of the reliability; a smaller value represented a more reliable measurement [27]. Univariable and multivariable linear regression analyses were performed to determine the significant factors affecting the QUS parameters. All statistical analyses were performed using MedCalc version 18.11.6 (MedCalc Software) and SPSS version 25.0 (IBM Corp.). A *p* value of < 0.05 was considered statistically significant.

RESULTS

Participant Characteristics

A total of 120 participants (75 males and 45 females; mean age, 49.1 ± 12.6 years), including 96 participants with known or clinically suspected NAFLD and 24 scheduled for liver donation, were included in the analysis. The participant characteristics are summarized in Table 1. The mean MRI-PDFF was 10.2% ± 7.1 (range, 1–37.7%); 38, 23, and 59 participants had MRI-PDFFs of < 5%, 5–10%, ≥ 10%, respectively. Based on the MRE results, 3.3% (4 of 120) of patients were categorized as having ≥ F2. The median interval between US and MRI was 0 days (range, 0–14 days), given that 80.0% of participants (96 of 120) underwent both examinations on the same day.

https://doi.org/10.3348/kjr.2020.1262

Korean Journal of Radiology
KJR

Correlation between QUS Parameters and MRI-PDFF

Both AC-TAI and SC-TSI showed significant positive correlations with MRI-PDFF (r = 0.659 and 0.727; 95% confidence interval [CI] = 0.544–0.750 and 0.630–0.802; p < 0.001 for both). The distribution of AC-TAI and SC-TSI across the different categories of hepatic fat content assessed with MRI-PDFF is presented in Figure 3 and Table 2. Both AC-TAI and SC-TSI showed significant differences based on their hepatic steatosis grades (p < 0.001).

Table 1. Patient Characteristics

Variable	Value (n = 120)
Age, years	49.1 ± 12.6 (20–73)
Sex	
Male	75 (62.5)
Female	45 (37.5)
BMI, kg/m^2	26.1 ± 3.5 (18.1–37.2)
Skin-to-liver capsule distance, mm	19.2 ± 3.9 (11–36)
Aspartate aminotransferase, IU/L	37.3 ± 34.6 (12–258)
Alanine aminotransferase, IU/L	45.5 ± 42.0 (9–313)
Hepatic fibrosis grades	
< F2 (without significant fibrosis)	106 (88.3)
≥ F2 (with significant fibrosis)	14 (11.7)
Visual hepatic steatosis grade	
S0	49 (40.8)
S1	28 (23.3)
S2	30 (25.0)
S3	13 (10.8)
MRI-PDFF, %	10.2 ± 7.1 (1–37.7)
< 5	38 (31.7)
≥ 5 to < 10	23 (19.2)
≥ 10	59 (49.2)

Values are presented as mean ± standard deviation (range) or number (%) as appropriate. BMI = body mass index, MRI-PDFF = magnetic resonance imaging proton density fat fraction

Diagnostic Performance of QUS Parameters for Hepatic Steatosis

The AUCs of AC-TAI and SC-TSI for the detection of hepatic fat content of ≥ 5% (MRI-PDFF ≥ 5%) were 0.861 (95% CI: 0.786–0.918) and 0.964 (95% CI: 0.913–0.989) at the cutoff values of 0.884 and 91.2, respectively (Fig. 4). For detecting hepatic fat content of ≥ 5%, an AC-TAI of > 0.884 dB/cm/MHz had a sensitivity of 78.0% (64/82) and specificity of 78.9% (30/38), whereas an SC-TSI of > 91.2 had a sensitivity of 85.4% (70/82) and specificity of 97.4% (37/38).

The AUCs of AC-TAI and SC-TSI for the detection of hepatic fat content of ≥ 10% (MRI-PDFF ≥ 10%) were 0.835 (95% CI: 0.757–0.897) and 0.935 (95% CI: 0.875–0.972) at cutoff values of 0.980 dB/cm/MHz and 94.0, respectively (Fig. 4). The corresponding sensitivity, specificity, positive predictive value, and negative predictive value are shown in Table 3.

For the detection of hepatic fat contents of ≥ 5% and ≥ 10%, SC-TSI showed significantly higher AUCs than the visual steatosis grades (p < 0.001 and p = 0.026, respectively); there was no statistically significant difference between the AUCs of AC-TAI and visual steatosis grades (p = 0.072 and p = 0.763, respectively).

Factors Associated with QUS Parameters

Univariable linear regression analysis showed that body mass index (BMI), skin-liver capsule distance, and MRI-PDFF were significant factors affecting AC-TAI. In addition, BMI, skin-liver capsule distance, alanine aminotransferase, and MRI-PDFF significantly affected SC-TSI. Multivariable analysis showed that MRI-PDFF was an independent

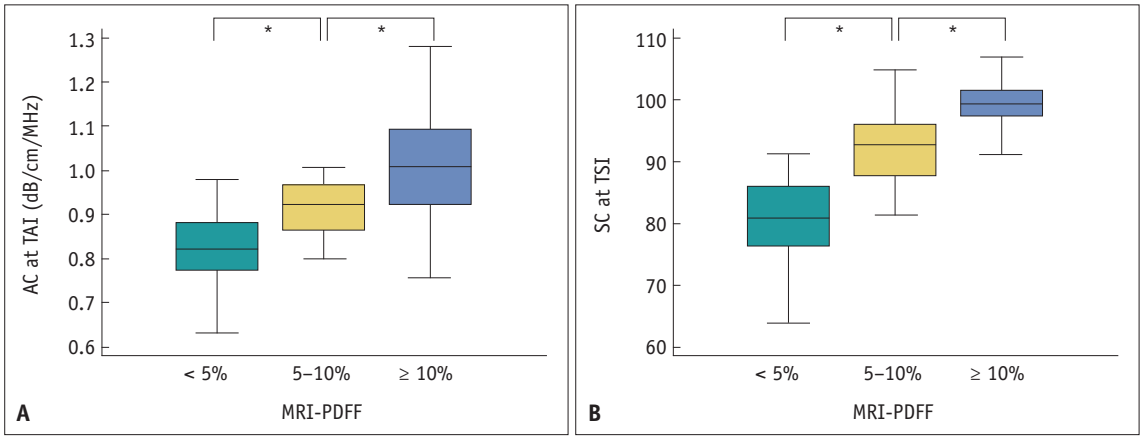

Fig. 3. The distribution of at AC-TAI (A) and SC-TSI (B) are stratified by hepatic fat content on MRI-PDFF. *Statistical significance. AC = attenuation coefficient, MRI-PDFF = magnetic resonance imaging proton density fat fraction, SC = scatter-distribution coefficient, TAI = tissue attenuation imaging, TSI = tissue scatter-distribution imaging

https://doi.org/10.3348/kjr.2020.1262

Table 2. Quantitative US Parameters According to Hepatic Steatosis Grades

Quantitative US Parameters	Hepatic Steatosis Grade			*P*		
	MRI-PDFF < 5% (n = 38)	MRI-PDFF 5–10% (n = 23)	MRI-PDFF ≥ 10% (n = 59)	Kruskal-Wallis Test	Dunn's Post Hoc Test	
					< 5% vs. 5–10%	5–10% vs. ≥ 10%
AC at TAI, dB/cm/MHz	0.829 ± 0.085	0.915 ± 0.063	1.006 ± 0.119	< 0.001	0.013	0.015
SC at TSI	80.3 ± 7.3	91.9 ± 5.5	98.7 ± 4.7	< 0.001	0.001	0.001

Values are presented as mean ± standard deviation unless otherwise specified. AC = attenuation coefficient, MRI-PDFF = magnetic resonance imaging proton density fat fraction, SC = scatter-distribution coefficient, TAI = tissue attenuation imaging, TSI = tissue scatter-distribution imaging, US = ultrasound

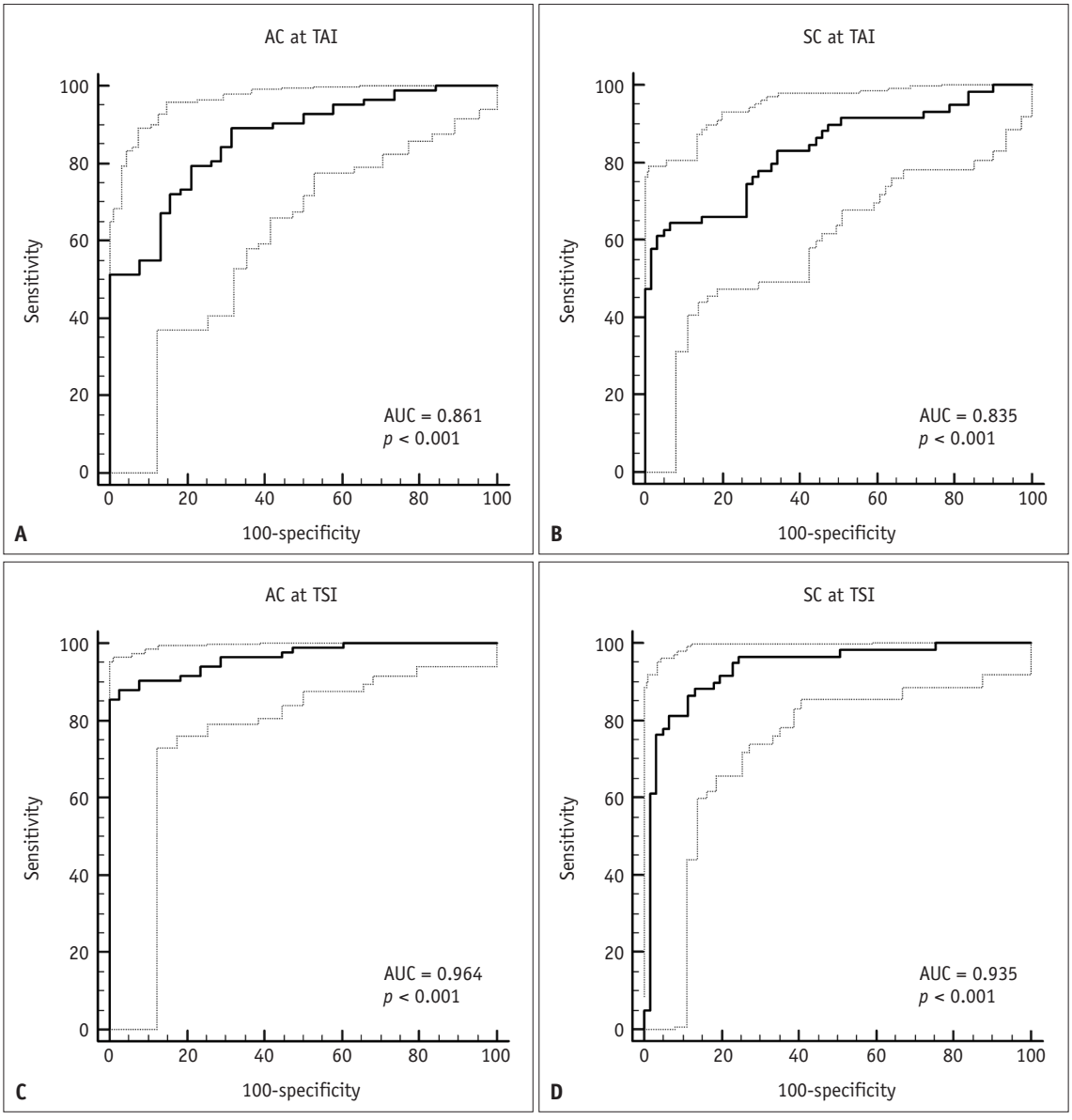

Fig. 4. The diagnostic performances of AC at TAI (A, C) and SC at TSI (B, D) for the detection of hepatic steatosis (MRI-PDFF ≥ 5%; A, B) and the detection of hepatic fat contents of ≥ 10% (MRI-PDFF ≥ 10%; C, D). AC = attenuation coefficient, AUC = area under the receiver operating characteristic curve, MRI-PDFF = magnetic resonance imaging proton density fat fraction, SC = scatter-distribution coefficient, TAI = tissue attenuation imaging, TSI = tissue scatter-distribution imaging

https://doi.org/10.3348/kjr.2020.1262

Korean Journal of Radiology
KJR

determinant for AC-TAI and SC-TSI, and it was positively correlated with both (p < 0.001) (Table 4).

Reproducibility of QUS Parameters

The inter-examination repeatability of SC-TSI was excellent with an ICC of 0.959 (95% CI: 0.941–0.971) and CV of 3.3% (95% CI: 2.9–3.7), and that of AC-TAI was good with an ICC of 0.892 (95% CI: 0.844–0.924) and CV of 6.7% (95% CI: 5.8–7.6).

DISCUSSION

In our study, the QUS parameters (AC at TAI and SC at TSI) showed a good correlation with MRI-PDFF (r = 0.659

Table 3. Diagnostic Performance of Quantitative US Parameters and Visual Grade for the Detection of Hepatic Steatosis

US Parameters	Hepatic Fat Content	AUC (95% CI)	Cutoff Value	Sensitivity*	Specificity*	PPV*	NPV*
Quantitative US parameters							
AC at TAI, dB/cm/MHz	MRI-PDFF ≥ 5%	0.861 (0.786–0.918)	> 0.884	78.0 (64/82)	78.9 (30/38)	88.9 (64/72)	62.5 (30/48)
	MRI-PDFF ≥ 10%	0.835 (0.757–0.897)	> 0.980	64.4 (38/59)	93.4 (57/61)	90.5 (38/42)	73.1 (57/78)
SC at TSI	MRI-PDFF ≥ 5%	0.964 (0.913–0.989)	> 91.2	85.4 (70/82)	97.4 (37/38)	98.6 (70/71)	75.5 (37/49)
	MRI-PDFF ≥ 10%	0.935 (0.875–0.972)		88.1 (52/59)	86.9 (53/61)	86.7 (52/60)	88.3 (53/60)
Visual steatosis grade	MRI-PDFF ≥ 5%	0.779 (0.694–0.850)	≥ S1 (mild)	76.8 (63/82)	79.0 (30/38)	88.7 (63/71)	61.2 (30/49)
	MRI-PDFF ≥ 10%	0.848 (0.771–0.907)	≥ S2 (moderate)	71.2 (42/59)	98.4 (60/61)	97.7 (42/43)	77.9 (60/77)

*Data in parentheses are number of patients. AC = attenuation coefficient, AUC = area under the receiver operating characteristic curve, MRI-PDFF = magnetic resonance imaging proton density fat fraction, NPV = negative predictive value, PPV = positive predictive value, SC = scatter-distribution coefficient, TAI = tissue attenuation imaging, TSI = tissue scatter-distribution imaging, US = ultrasound

Table 4. Univariable and Multivariable Linear Regression Analysis for Analyzing Factors Associated with Quantitative US Parameters

Parameter	Univariable Analysis		Multivariable Analysis	
	Coefficient (95% CI) (x 10^{-3})	P	Coefficient (95% CI) (x 10^{-3})	P
AC at TAI, dB/cm/MHz				
Female gender	-2 (-49, 46)	0.941		
Age, years	1 (-0.1, 3)	0.152		
BMI, kg/m^2	13 (7, 19)	< 0.001	0.1 (-7. 7)	0.944
Skin-liver capsule distance, mm	10 (4, 15)	0.001	3 (-1, 8)	0.146
Aspartate aminotransferase, IU/L	-0.9 (-1, 1)	0.782		
Alanine aminotransferase, IU/L	0.5 (-0.1, 1)	0.125		
MRI-PDFF, %	12 (9, 14)	< 0.001	12 (8, 14)	< 0.001
LS at MRE, kPa	23 (-9, 55)	0.150		
SC at TSI				
Female gender	-42 (-78, 5)	0.250		
Age, years	2 (-1, 3)	0.132		
BMI, kg/m^2	13 (9, 18)	< 0.001	5 (-0.3, 10)	0.072
Skin-liver capsule distance, mm	8 (4, 12)	< 0.001	1 (-0.4, 5)	0.858
Aspartate aminotransferase, IU/L	0.3 (-0.2, 1)	0.300		
Alanine aminotransferase, IU/L	0.6 (0.1, 1)	0.007	0.1 (-0.3, 0.6)	0.924
MRI-PDFF, %	10 (8, 12)	< 0.001	9 (7, 11)	< 0.001
LS at MRE, kPa	22 (-3, 47)	0.080		

AC = attenuation coefficient, BMI = body mass index, CI = confidence interval, LS = liver stiffness, MRE = magnetic resonance elastography, MRI-PDFF = magnetic resonance imaging proton density fat fraction, SC = scatter-distribution coefficient, TAI = tissue attenuation imaging, TSI = tissue scatter-distribution imaging, US = ultrasound

https://doi.org/10.3348/kjr.2020.1262

and $r = 0.727$; $p < 0.001$ for both) and good diagnostic performance for detecting and grading hepatic steatosis in patients with NAFLD using MRI-PDFF as a standard of reference. Additionally, multivariable linear regression analysis revealed that hepatic fat content assessed by MRI-PDFF was a significant determinant for AC-TAI and SC-TSI. Moreover, their measurements showed good inter-examination repeatability. US beam attenuation increases with depth, which correlates with an increase in AC-TAI [28]. In addition, as fat droplets create acoustic scattering in the liver parenchyma, the US backscattered statistics shift from pre- to post-Rayleigh, which increases its SC-TSI [29]. This may account for the significant positive correlation between both QUS parameters and MRI-PDFF in our study. Considering the significant correlation between QUS parameters and MRI-PDFF obtained in our study and the good inter-exam repeatability, QUS parameters could help assess hepatic steatosis as a noninvasive and widely available diagnostic tool.

In our study, both QUS parameters showed good diagnostic performance for detecting hepatic fat content of ≥ 5%. AC-TAI had a sensitivity of 78.1% and specificity of 79.0%, whereas SC-TSI had a sensitivity of 85.4% and specificity of 97.4%. Moreover, AC-TAI and SC-TSI had balanced sensitivity and specificity (sensitivity of 64.4% and 88.1%, and specificity of 93.4% and 86.9%, respectively) for the detection of hepatic fat contents of ≥ 10%. These results are consistent with previous studies that showed a good diagnostic performance for US attenuation or backscatter in patients with NAFLD [12,13]. Although MR-based fat quantification is currently accepted as the noninvasive reference standard for hepatic fat quantification [9,30], it is limited by its high cost and limited accessibility. We believe that US-based technologies such as QUS may be a promising first-line tool for assessing hepatic steatosis in patients with NAFLD [14]. Our results suggest the potential application of AC-TAI and SC-TSI for screening for hepatic steatosis in patients with clinically suspected NAFLD.

In our study, SC-TSI showed significantly better diagnostic performance for the detection of hepatic fat contents of ≥ 5% and ≥ 10%, which was consistent with the report of a previous study [15]. On the contrary, although the AUCs of AC-TAI were higher than those of the visual steatosis grades, the difference was not statistically significant in our study. A previous study reported that AC had a better diagnostic performance than the visual steatosis grades [15]. QUS parameters may be useful for the evaluation of the hepatic fat content by providing objective continuous values, whereas visual assessment provides only subjective categorical values. The application of QUS parameters may be clinically useful for the screening of hepatic steatosis, longitudinal follow-up, and the evaluation of treatment response in patients with hepatic steatosis.

Multivariable linear regression analysis showed that MRI-PDFF was an independent determinant for both AC-TAI and SC-TSI (both p values of < 0.001). Meanwhile, LS detected by MRE, which indicates the degree of hepatic fibrosis, did not show a significant relationship with AC-TAI and SC-TSI. In previous studies, hepatic fibrosis showed a negative relationship with SC-TSI (reflecting the Nakagami parameter) [15,31,32], which was contrary to our results. Whereas normal parenchymal tissue showed a near-Rayleigh distribution due to randomly distributed scatterers, the liver parenchymal tissue with fibrotic structures or nodules (resolvable scatterers) tends to demonstrate more of a pre-Rayleigh distribution, resulting in a decrease in the SC-TSI [32]. However, LS detected on MRE did not show a significant relationship with SC-TSI in our study. This difference could be associated with the characteristics of the study population, as our study population had only a small percentage of patients with significant fibrosis (11.7%, 14/120), there could be a limitation in evaluating the relationship between QUS parameters and hepatic fibrosis.

Meanwhile, there are some controversies regarding the relationship between hepatic fibrosis and AC-TAI (US attenuation). A previous study suggested that hepatic fibrosis showed a positive correlation with US attenuation [33]. However, another study showed no significant relationship [34], and this was consistent with our study result. Theoretically, attenuation of the US beam could be affected by fibrosis, although its effect is less than that of steatosis [35]. In our study, MRE was performed for all the study participants, and the AC-TAI was explained by the study population deviation, with only a small percentage with significant fibrosis according to the MRE stiffness values. However, considering the small number of patients with significant fibrosis, further studies involving those with various stages of fibrosis may facilitate the precise evaluation of the relationship between hepatic fibrosis and QUS parameters.

Our study has several limitations. First, the study population was biased toward NAFLD, as only 31.7% of the

https://doi.org/10.3348/kjr.2020.1262

Korean Journal of Radiology
KJR

patients were normal (MRI-PDFF < 5%); this is different from the prevalence in the general population. Second, although the QUS technique based on RF data analysis can be implemented in clinical US systems, it is not readily available in all clinical US systems. However, with most manufacturers beginning to provide RF output capabilities, it may be widely available in the near future.

In conclusion, AC-TAI and SC-TSI derived from QUS RF data analysis yielded good correlations with MRI-PDFF and provided good performance for detecting hepatic steatosis and assessing its severity in NAFLD.

Supplement

The Data Supplement is available with this article at https://doi.org/10.3348/kjr.2020.1262.

Conflicts of Interest

Jeong Min Lee received grants from Samsung Medison for this study; personal fees and non-financial support from Siemens Healthcare, grants from RF MEDICAL, grants and personal fees from Bayer Healthcare, grants and personal fees from Guerbet, grants from Philips Healthcare, grants from GE Healthcare, and grants from Canon Medical, outside the submitted work. Sun Kyung Jeon, Ijin Joo, and Sae Jin Park: no conflicts of interest.

Author Contributions

Conceptualization: Ijin Joo, Jeong Min Lee. Data curation: Sun Kyung Jeon, Ijin Joo, Sae-Jin Park. Formal analysis: Sun Kyung Jeon. Funding acquisition: Jeong Min Lee. Investigation: Sun Kyung Jeon, Ijin Joo, Jeong Min Lee. Methodology: Sun Kyung Jeon, Jeong Min Lee. Supervision: Jeong Min Lee. Writing—original draft: Sun Kyung Jeon. Writing—review & editing: all authors.

ORCID iDs

Sun Kyung Jeon
https://orcid.org/0000-0002-8991-3986
Jeong Min Lee
https://orcid.org/0000-0003-0561-8777
Ijin Joo
https://orcid.org/0000-0002-1341-4072
Sae-Jin Park
https://orcid.org/0000-0001-8580-3272

REFERENCES

1. Castera L, Friedrich-Rust M, Loomba R. Noninvasive assessment of liver disease in patients with nonalcoholic fatty liver disease. *Gastroenterology* 2019;156:1264-1281.e4
2. Vernon G, Baranova A, Younossi ZM. Systematic review: the epidemiology and natural history of non-alcoholic fatty liver disease and non-alcoholic steatohepatitis in adults. *Aliment Pharmacol Ther* 2011;34:274-285
3. Friedman SL, Neuschwander-Tetri BA, Rinella M, Sanyal AJ. Mechanisms of NAFLD development and therapeutic strategies. *Nat Med* 2018;24:908-922
4. Pais R, Barritt AS 4th, Calmus Y, Scatton O, Runge T, Lebray P, et al. NAFLD and liver transplantation: current burden and expected challenges. *J Hepatol* 2016;65:1245-1257
5. Machado MV, Cortez-Pinto H. Non-invasive diagnosis of non-alcoholic fatty liver disease. A critical appraisal. *J Hepatol* 2013;58:1007-1019
6. Reeder SB, Cruite I, Hamilton G, Sirlin CB. Quantitative assessment of liver fat with magnetic resonance imaging and spectroscopy. *J Magn Reson Imaging* 2011;34:729-749
7. Tang A, Desai A, Hamilton G, Wolfson T, Gamst A, Lam J, et al. Accuracy of MR imaging-estimated proton density fat fraction for classification of dichotomized histologic steatosis grades in nonalcoholic fatty liver disease. *Radiology* 2015;274:416-425
8. Yokoo T, Serai SD, Pirasteh A, Bashir MR, Hamilton G, Hernando D, et al. Linearity, bias, and precision of hepatic proton density fat fraction measurements by using MR imaging: a meta-analysis. *Radiology* 2018;286:486-498
9. Kramer H, Pickhardt PJ, Kliewer MA, Hernando D, Chen GH, Zagzebski JA, et al. Accuracy of liver fat quantification with advanced CT, MRI, and ultrasound techniques: prospective comparison with MR spectroscopy. *AJR Am J Roentgenol* 2017;208:92-100
10. Zhou Z, Zhang Q, Wu W, Lin YH, Tai DI, Tseng JH, et al. Hepatic steatosis assessment using ultrasound homodyned-K parametric imaging: the effects of estimators. *Quant Imaging Med Surg* 2019;9:1932-1947
11. Dasarathy S, Dasarathy J, Khiyami A, Joseph R, Lopez R, McCullough AJ. Validity of real time ultrasound in the diagnosis of hepatic steatosis: a prospective study. *J Hepatol* 2009;51:1061-1067
12. Lin SC, Heba E, Wolfson T, Ang B, Gamst A, Han A, et al. Noninvasive diagnosis of nonalcoholic fatty liver disease and quantification of liver fat using a new quantitative ultrasound technique. *Clin Gastroenterol Hepatol* 2015;13:1337-1345.e6
13. Paige JS, Bernstein GS, Heba E, Costa EAC, Fereirra M, Wolfson T, et al. A pilot comparative study of quantitative ultrasound, conventional ultrasound, and MRI for predicting histology-determined steatosis grade in adult nonalcoholic fatty liver disease. *AJR Am J Roentgenol* 2017;208:W168-W177
14. Yang KC, Liao YY, Tsui PH, Yeh CK. Ultrasound imaging in nonalcoholic liver disease: current applications and future

developments. *Quant Imaging Med Surg* 2019;9:546-551
15. Jeon SK, Joo I, Kim SY, Jang JK, Park J, Park HS, et al. Quantitative ultrasound radiofrequency data analysis for the assessment of hepatic steatosis using the controlled attenuation parameter as a reference standard. *Ultrasonography* 2021;40:136-146
16. Hamaguchi M, Kojima T, Itoh Y, Harano Y, Fujii K, Nakajima T, et al. The severity of ultrasonographic findings in nonalcoholic fatty liver disease reflects the metabolic syndrome and visceral fat accumulation. *Am J Gastroenterol* 2007;102:2708-2715
17. Reeder SB, Robson PM, Yu H, Shimakawa A, Hines CD, McKenzie CA, et al. Quantification of hepatic steatosis with MRI: the effects of accurate fat spectral modeling. *J Magn Reson Imaging* 2009;29:1332-1339
18. Hamilton G, Yokoo T, Bydder M, Cruite I, Schroeder ME, Sirlin CB, et al. In vivo characterization of the liver fat ^{1}H MR spectrum. *NMR Biomed* 2011;24:784-790
19. Tang A, Tan J, Sun M, Hamilton G, Bydder M, Wolfson T, et al. Nonalcoholic fatty liver disease: MR imaging of liver proton density fat fraction to assess hepatic steatosis. *Radiology* 2013;267:422-431
20. Han A, Zhang YN, Boehringer AS, Montes V, Andre MP, Erdman JW Jr, et al. Assessment of hepatic steatosis in nonalcoholic fatty liver disease by using quantitative US. *Radiology* 2020;295:106-113
21. Caussy C, Alquiraish MH, Nguyen P, Hernandez C, Cepin S, Fortney LE, et al. Optimal threshold of controlled attenuation parameter with MRI-PDFF as the gold standard for the detection of hepatic steatosis. *Hepatology* 2018;67:1348-1359
22. Lee DH, Lee JM, Yi NJ, Lee KW, Suh KS, Lee JH, et al. Hepatic stiffness measurement by using MR elastography: prognostic values after hepatic resection for hepatocellular carcinoma. *Eur Radiol* 2017;27:1713-1721
23. Yoon JH, Lee JM, Woo HS, Yu MH, Joo I, Lee ES, et al. Staging of hepatic fibrosis: comparison of magnetic resonance elastography and shear wave elastography in the same individuals. *Korean J Radiol* 2013;14:202-212
24. Singh S, Venkatesh SK, Loomba R, Wang Z, Sirlin C, Chen J, et al. Magnetic resonance elastography for staging liver fibrosis in non-alcoholic fatty liver disease: a diagnostic accuracy systematic review and individual participant data pooled analysis. *Eur Radiol* 2016;26:1431-1440
25. Youden WJ. Index for rating diagnostic tests. *Cancer* 1950;3:32-35
26. Koo TK, Li MY. A guideline of selecting and reporting intraclass correlation coefficients for reliability research. *J Chiropr Med* 2016;15:155-163
27. Bland JM, Altman DG. Statistical methods for assessing agreement between two methods of clinical measurement. *Lancet* 1986;1:307-310
28. Kim H, Varghese T. Attenuation estimation using spectral cross-correlation. *IEEE Trans Ultrason Ferroelectr Freq Control* 2007;54:510-519
29. Wan YL, Tai DI, Ma HY, Chiang BH, Chen CK, Tsui PH. Effects of fatty infiltration in human livers on the backscattered statistics of ultrasound imaging. *Proc Inst Mech Eng H* 2015;229:419-428
30. Gu J, Liu S, Du S, Zhang Q, Xiao J, Dong Q, et al. Diagnostic value of MRI-PDFF for hepatic steatosis in patients with non-alcoholic fatty liver disease: a meta-analysis. *Eur Radiol* 2019;29:3564-3573
31. Tsui PH, Ho MC, Tai DI, Lin YH, Wang CY, Ma HY. Acoustic structure quantification by using ultrasound Nakagami imaging for assessing liver fibrosis. *Sci Rep* 2016;6:33075
32. Yamada H, Ebara M, Yamaguchi T, Okabe S, Fukuda H, Yoshikawa M, et al. A pilot approach for quantitative assessment of liver fibrosis using ultrasound: preliminary results in 79 cases. *J Hepatol* 2006;44:68-75
33. Jeon SK, Lee JM, Joo I, Yoon JH, Lee DH, Lee JY, et al. Prospective evaluation of hepatic steatosis using ultrasound attenuation imaging in patients with chronic liver disease with magnetic resonance imaging proton density fat fraction as the reference standard. *Ultrasound Med Biol* 2019;45:1407-1416
34. Tada T, Kumada T, Toyoda H, Yasuda S, Sone Y, Hashinokuchi S, et al. Liver stiffness does not affect ultrasound-guided attenuation coefficient measurement in the evaluation of hepatic steatosis. *Hepatol Res* 2020;50:190-198
35. Lin T, Ophir J, Potter G. Correlation of ultrasonic attenuation with pathologic fat and fibrosis in liver disease. *Ultrasound Med Biol* 1988;14:729-734

https://doi.org/10.3348/kjr.2020.1262